A NEW HYDROSTATIC RECONSTRUCTION SCHEME BASED ON SUBCELL RECONSTRUCTIONS[*]

GUOXIAN CHEN[†] AND SEBASTIAN NOELLE[‡]

Abstract. A key difficulty in the analysis and numerical approximation of the shallow water equations is the nonconservative product of measures due to the gravitational force acting on a sloped bottom. Solutions may be nonunique, and numerical schemes are not only consistent discretizations of the shallow water equations, but they also determine how to model the physics. Our derivation is based on a subcell reconstruction using infinitesimal singular layers at the cell boundaries, as inspired by S. Noelle, Y. Xing, and C.-W. Shu [*J. Comput. Phys.*, 226 (2007), pp. 29–58]. One key step is to separate the singular measures. Another aspect is the reconstruction of the solution variables in the singular layers. We study three reconstructions. The first leads to the well-known scheme of Audusse et al., [*SIAM J. Sci. Comput.*, 25 (2004), pp. 2050–2065], which introduces the hydrostatic reconstruction. The second is a modification proposed in [T. Morales de Luna, M. J. Castro Díaz, and C. Parés, *Appl. Math. Comput.*, 219 (2013), pp. 9012–9032], which analyzes whether a wave has enough energy to overcome a step. The third is our new scheme, which borrows its structure from the wet-dry front. For a number of cases discussed in recent years, where water runs down a hill, Audusse's scheme converges slowly or fails. Morales' scheme gives a visible improvement. Both schemes are clearly outperformed by our new scheme.

Key words. shallow water equations, water at rest, well-balanced property, wet-dry front, semi discrete entropy inequality, nonconservative products of measures

AMS subject classifications. 76M12, 35L65

DOI. 10.1137/15M1053074

1. Introduction. In this paper, we consider a class of finite volume schemes for the shallow water equations with variable bottom topography. These equations are a prototype of hyperbolic balance laws.

Balance laws often consist of the conservation laws for the vector $U(x,t)$ of mass and momentum, accelerated by conservative advection and pressure forces (denoted by $-\partial F(U)/\partial x$ in (1.1) below), and by additional nonconservative forces $S(U,x)$, also called source terms. Hence the equations of motion may be written as

$$(1.1) \qquad \frac{\partial U}{\partial t} + \frac{\partial F(U)}{\partial x} = S(U,x).$$

In this paper, there is no source term in the equation of mass, so we can write $S = (0,s)^T$.

A particular challenge is the analytical and numerical understanding of near-equilibrium flows, for which the residuum

[†]Computational Science Hubei Key Laboratory, School of Mathematics and Statistics, Wuhan University, Wuhan 430072, People's Republic of China (gxchen.math@whu.edu.cn).

[‡]Institute for Geometry and Practical Mathematics, RWTH Aachen University, Templergraben 55, 52062 Aachen, Germany (noelle@igpm.rwth-aachen.de).

(1.2)
$$R(x,t) := -\frac{\partial F(U)}{\partial x} + S(U,x)$$

nearly vanishes.

A semidiscrete, first order accurate finite volume scheme may be written as a method of lines

(1.3)
$$\frac{d}{dt}U_i(t) = R_i(t) := -\frac{1}{\Delta x}\left(F_{i+\frac{1}{2}} - F_{i-\frac{1}{2}}\right) + S_i,$$

where $U_i(t)$ approximates the cell average over cell $C_i = [x_{i-\frac{1}{2}}, x_{i+\frac{1}{2}}]$ at time t, $R_i(t)$ is the cell average of the residuum, $\Delta x = x_{i+\frac{1}{2}} - x_{i-\frac{1}{2}}$ is the spatial grid size, $F_{i\pm 1/2}$ is a conservative numerical flux function, and S_i approximates the cell average of the source term. Lax and Wendroff proved in 1960 that limits of conservative numerical schemes are weak solutions of the corresponding systems of hyperbolic conservation laws [14]. There are many well-established conservative numerical fluxes (usually called approximate Riemann solvers); see, e.g., [21, 12, 22, 6, 11] and the references therein. On the other hand, there is no general procedure to discretize the source term.

Indeed, it is a challenge for each balance law, each equilibrium state, and each numerical flux function to find a discretization of the source which preserves desirable stability properties. There is, however, one common feature to most balance laws: since the force in Newton's law equals mass times acceleration, the source term $S(U,x)$ is often a product term. Each of the factors may become a singular measure at the cell boundaries, and sometimes their product cannot be evaluated. In [9], Dal Maso, LeFloch, and Murat presented a theory of nonconservative products of measures. This was systematically extended to a numerical framework of path-conservative schemes by Parés and Castro et al. (see [20, 7]). However, the limits of these schemes are not unique, and any choice of path implies a—perhaps tacit modeling assumption (see the discussion in [8, 1, 16]).

In this work, we focus on the one-dimensional shallow water equations, given by

(1.4)
$$U = \begin{pmatrix} h \\ hu \end{pmatrix}, \quad F(U) = \begin{pmatrix} hu \\ hu^2 + \frac{1}{2}gh^2 \end{pmatrix}, \quad \text{and} \quad S(U,x) = -\begin{pmatrix} 0 \\ ghz_x \end{pmatrix}.$$

Here $z(x)$ is the bottom topography, $h(x,t)$ the water depth, $u(x,t)$ the water velocity, and $g = 9.8\text{m/s}^2$ the gravitational acceleration. Thus the source term models the force of gravity tangential to a sloped bottom. It is instructive to rewrite the residuum as

(1.5)
$$R = -\begin{pmatrix} hu \\ hu^2 \end{pmatrix}_x - gh\begin{pmatrix} 0 \\ w \end{pmatrix}_x,$$

where $w = z + h$ is the water level. Two important equilibria are

(i) *still water*, where

(1.6)
$$u = 0 \text{ and } w_x = 0, \text{and}$$

(ii) the *lake at rest*, which is still water together with dry boundaries:

(1.7)
$$u = 0 \text{ and } hw_x = 0.$$

Hence the lake at rest residuum combines the dry shore ($h = 0$) with the flat water level ($w_x = 0$) in a single product. This expression also suggests a natural splitting of the nonconservative product at the wet-dry front.

Well-balanced schemes, which preserve the lake at rest discretely, use either continuous or discontinuous topography. Here we consider schemes using a piecewise constant bottom, such as [3, 4, 2, 7, 17, 18] and the references therein. These are particularly simple to implement, especially in two space dimensions, but they have to cope with the notorious difficulty of discontinuous measures. In particular, we focus on Audusse's well-known hydrostatic reconstruction (HR) scheme [2], which is well-balanced, positivity preserving, and satisfies a semidiscrete entropy inequality.

A key contribution of the present work is the analysis of the existing, and the derivation of a new, HR scheme using subcell reconstructions. In two infinitesimal layers adjacent to each edge, we reconstruct the bottom topography as a continuous, piecewise linear function (see section 3.2). In a next step the water level and velocity are reconstructed (see section 3.3). Based on these, the numerical fluxes, residual, and update can be computed directly. In Theorem 3.5 we prove that the schemes based on subcell reconstructions coincide with the original HR schemes.

More importantly, the study of infinitesimal layers helps to uncover a defect of the original HR scheme, and motivates the construction of an improved scheme. The crucial case is the partially wet interface studied in Figure 3. Here the subcell reconstruction reveals an infinitesimal region of vacuum for Audusse's scheme, in a situation where a continuous linear bottom should actually be covered by water. This has a remarkable physical consequence: due to the vacuum, part of the bottom slope does not contribute to the gravitational acceleration. This, and only this, is the reason that downward flows computed by Audusse's scheme lag behind in some of the numerical experiments in section 5. Thus, the subcell reconstruction helps to visualize and analyze a deficiency of the scheme.

On the other hand, the subcell reconstruction facilitates the correction Audusse's scheme. As seen in the bottom-right part of Figure 3, the interface is now positioned at the wet-dry front, and it splits the source term according to (1.7). This ensures full physical acceleration, and leads to superior results in section 5.

The paper is organized as follows. In section 2, we summarize two known [2, 15] HR schemes and a new one. In section 3 we rederive the three HR methods using subcell reconstructions. In section 4, we establish the stability of the new HR scheme: positivity of the water height, well-balanced property for the lake at rest, and a semidiscrete entropy inequality. In section 5, several numerical experiments allow us to compare the three HR schemes. Some concluding remarks are made in section 6. Finally, in Appendix A, we give a summary from which the new HR scheme may be implemented directly.

2. Definition of the HR schemes. In this section, we summarize the three HR schemes. Each of them introduces reconstructed values $U_{i+\frac{1}{2}\pm}$ of the unknowns to the left and right of interface $x_{i+\frac{1}{2}}$, and defines the numerical flux via a Riemann solver $\mathcal{F}$:

$$F_{i+\frac{1}{2}} = \mathcal{F}(U_{i+\frac{1}{2}-}, U_{i+\frac{1}{2}+}).$$

Then the schemes split the singular source term at the interface into a left and a right part, $S_{i+\frac{1}{2}-}$ and $S_{i+\frac{1}{2}+}$, and compute the source term in (1.3) as

$$(2.1) \qquad S_i = S_{i-\frac{1}{2}+} + S_{i+\frac{1}{2}-} = \left(0, s_{i-\frac{1}{2}+}\right)^T + \left(0, s_{i+\frac{1}{2}-}\right)^T.$$

A key ingredient of this splitting is the definition of an intermediate bottom level $z_{i+\frac{1}{2}}$ at the interface.

There will be two main types of interface, depending on how the water covers the bottom to the left and right sides of the interface (see Figure 1). First, there is the
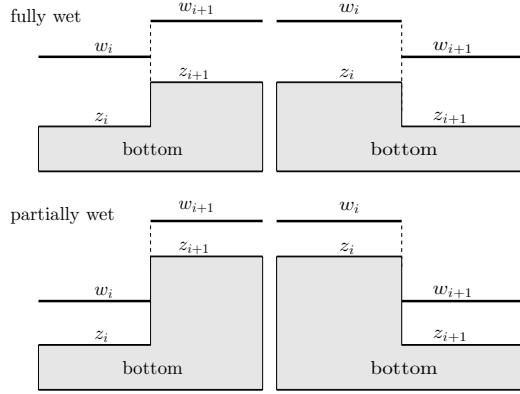
FIG. 1. *Examples of interfaces: fully wet (top), and partially wet (bottom).*

fully wet interface, where the water level on each side is higher than the higher side of the bottom topography:

$$(2.2) \qquad \min(w_i, w_{i+1}) > \max(z_i, z_{i+1}),$$

where z_i and $w_i = z_i + h_i$ are the bottom topography and the water level, respectively, in cell C_i. Second, there is the *partially wet interface*, where the water level on one side is equal to or below the topography on the other side:

$$(2.3) \qquad \min(w_i, w_{i+1}) \leq \max(z_i, z_{i+1}).$$

In the following, we distinguish the three HR schemes by superscripts, e.g., $h^{\mathrm{AUD}}_{i+\frac{1}{2}\pm}$, $h^{\mathrm{MOR}}_{i+\frac{1}{2}\pm}$, and $h^{\mathrm{CN}}_{i+\frac{1}{2}\pm}$ for the scheme of Audusse et al., the modification due to Morales et al., and the present scheme, respectively. After the water heights $h_{i-\frac{1}{2}+}$ and $h_{i+\frac{1}{2}-}$ are reconstructed, we define the conservative variables as

$$(2.4)$$
$$U_{i+\frac{1}{2}-} = \begin{pmatrix} h_{i+\frac{1}{2}-} \\ h_{i+\frac{1}{2}-}u_{i+\frac{1}{2}-} \end{pmatrix}, \ U_{i-\frac{1}{2}+} = \begin{pmatrix} h_{i-\frac{1}{2}+} \\ h_{i-\frac{1}{2}+}u_{i-\frac{1}{2}+} \end{pmatrix} \ \text{with } u_{i+\frac{1}{2}-} = u_{i-\frac{1}{2}+} = u_i.$$

Before we give a derivation of the method in terms of singular layers (see section 3), we first introduce the three HR schemes.

2.1. The original HR method. Audusse et al. [2] introduce their first order HR scheme by choosing the intermediate bottom as

$$(2.5) \qquad z^{\mathrm{AUD}}_{i+\frac{1}{2}} := \max(z_i, z_{i+1})$$

and the interface water heights as

$$(2.6) \qquad h^{\mathrm{AUD}}_{i+\frac{1}{2}-} := \max(w_i - z^{\mathrm{AUD}}_{i+\frac{1}{2}}, 0), \quad h^{\mathrm{AUD}}_{i+\frac{1}{2}+} := \max(w_{i+1} - z^{\mathrm{AUD}}_{i+\frac{1}{2}}, 0).$$

Then they discretize the source term as

$$(2.7) \qquad s^{\mathrm{AUD}}_{i+\frac{1}{2}-} := \frac{g}{2\Delta x}\left((h^{\mathrm{AUD}}_{i+\frac{1}{2}-})^2 - (h_i)^2\right),$$

$$(2.8) \qquad s^{\mathrm{AUD}}_{i+\frac{1}{2}+} := \frac{g}{2\Delta x}\left((h_{i+1})^2 - (h^{\mathrm{AUD}}_{i+\frac{1}{2}+})^2\right).$$

2.2. The HR method of Morales et al. The HR scheme of Morales et al. [15] is identical to that of Audusse's scheme,

$$(2.9) \qquad z_{i+\frac{1}{2}}^{\mathrm{MOR}} := z_{i+\frac{1}{2}}^{\mathrm{AUD}}, \quad h_{i+\frac{1}{2}-}^{\mathrm{MOR}} := h_{i+\frac{1}{2}-}^{\mathrm{AUD}}, \quad h_{i+\frac{1}{2}+}^{\mathrm{MOR}} := h_{i+\frac{1}{2}+}^{\mathrm{AUD}},$$

and the source term is defined as

$$(2.10) \qquad s_{i+\frac{1}{2}-}^{\mathrm{MOR}} := s_{i+\frac{1}{2}-}^{\mathrm{AUD}}, \quad s_{i+\frac{1}{2}+}^{\mathrm{MOR}} := s_{i+\frac{1}{2}+}^{\mathrm{AUD}},$$

except for the partially wet interfaces (2.3), where water either flows downhill or flows uphill with enough kinetic energy to climb the jump of the bottom at the interface. This results in the following two cases.

(i) $z_i < z_{i+1}$ (ascending bottom). If $u_i < 0$, or $u_i > 0$ and

$$(2.11) \qquad \frac{|u_i|^2}{2} + g(w_i - z_{i+1}) \geq \frac{3}{2}\sqrt{g(h_i|u_i|)^3},$$

then the left interface source term is redefined as

$$(2.12) \qquad s_{i+\frac{1}{2}-}^{\mathrm{MOR}} := -\frac{g}{\Delta x}\frac{h_i}{2}\left(z_{i+\frac{1}{2}}^{\mathrm{MOR}} - z_i\right).$$

(ii) $z_i > z_{i+1}$ (*descending bottom*). If $u_{i+1} > 0$, or $u_{i+1} < 0$ and

$$(2.13) \qquad \frac{|u_{i+1}|^2}{2} + g(w_{i+1} - z_i) \geq \frac{3}{2}\sqrt{g(h_{i+1}|u_{i+1}|)^3},$$

then the right interface source term is redefined as

$$(2.14) \qquad s_{i+\frac{1}{2}+}^{\mathrm{MOR}} := -\frac{g}{\Delta x}\frac{h_{i+1}}{2}\left(z_{i+1} - z_{i+\frac{1}{2}}^{\mathrm{MOR}}\right).$$

2.3. The present HR method. For the present HR method, the intermediate bottom is defined as

$$(2.15) \qquad z_{i+\frac{1}{2}}^{\mathrm{CN}} := \min\left(\max(z_i, z_{i+1}), \min(w_i, w_{i+1})\right).$$

The interface water heights are given by

$$(2.16) \qquad h_{i+\frac{1}{2}-}^{\mathrm{CN}} := \min(w_i - z_{i+\frac{1}{2}}^{\mathrm{CN}}, h_i), \quad h_{i+\frac{1}{2}+}^{\mathrm{CN}} := \min(w_{i+1} - z_{i+\frac{1}{2}}^{\mathrm{CN}}, h_{i+1}),$$

and the interface source terms are defined as

$$(2.17) \qquad s_{i+\frac{1}{2}-}^{\mathrm{CN}} := -\frac{g}{\Delta x}\frac{h_i + h_{i+\frac{1}{2}-}^{\mathrm{CN}}}{2}\left(z_{i+\frac{1}{2}}^{\mathrm{CN}} - z_i\right).$$

$$(2.18) \qquad s_{i+\frac{1}{2}+}^{\mathrm{CN}} := -\frac{g}{\Delta x}\frac{h_{i+\frac{1}{2}+}^{\mathrm{CN}} + h_{i+1}}{2}\left(z_{i+1} - z_{i+\frac{1}{2}}^{\mathrm{CN}}\right).$$

Remark 2.1. In Proposition 3.7, we state several relations between the three HR schemes. The most important is that for fully wet interfaces, all schemes are identical. The differences for the partially wet case are rather subtle, and the entire of section 3 is devoted to this. A quick look at Figure 3 may already give the reader an idea of the construction.

2.4. The numerical flux. In our computation we use Harten–Lax–van Leer (HLL)-type Riemann solvers,

$$(2.19) \qquad \mathcal{F}_{\mathrm{HLL}}(U_-, U_+) = \frac{s^+ F(U_-) - s^- F(U_+) + s^+ s^- (U_+ - U_-)}{s^+ - s^-},$$

where the smallest and largest wave speeds s^- and s^+ are chosen as

$$(2.20) \qquad s^- = \min(u_- - a_-, u_+ - a_+, 0), \quad s^+ = \max(u_- + a_-, u_+ + a_+, 0)$$

with gravitational wave speed $a = \sqrt{gh}$. For the stability analysis, we need two key inequalities satisfied by the HLL flux. The first one states that there is no numerical mass flux out of an empty cell, and is used in Theorem 4.1 to prove positivity of the water height.

LEMMA 2.2. *The first component of the HLL flux satisfies*

$$(2.21) \qquad \mathcal{F}^h(0, 0, h, hu)) \leq 0, \qquad \mathcal{F}^h(h, hu, 0, 0)) \geq 0.$$

This well-known property follows directly from the definition of the wave speeds (2.20). The second inequality is used in the proof of the semidiscrete entropy inequality in Theorem 4.6. It states that the numerical mass flux into a vacuum cell is at least as large as the physical mass flux.

LEMMA 2.3. *The first component of the HLL flux satisfies*

$$(2.22) \qquad \mathcal{F}^h(h, hu, 0, 0) - hu \geq 0, \qquad hu - \mathcal{F}^h(0, 0, h, hu) \geq 0.$$

Proof. The proof follows from (2.19) and (2.20) via

$$\mathcal{F}^h(h, hu, 0, 0) - hu = \frac{s^+ hu - s^+ s^- h}{s^+ - s^-} - hu = \frac{-s^- h(s^+ - u)}{s^+ - s^-} \geq 0,$$

$$hu - \mathcal{F}^h(0, 0, h, hu) = hu - \frac{-s^- hu + s^+ s^- h}{s^+ - s^-} = \frac{s^+ h(u - s^-)}{s^+ - s^-} \geq 0. \qquad \square$$

3. Interpretation via subcell reconstructions. In the present section, we rederive schemes of the form (1.3) by an infinitesimal limit process. The advantage of this process is that it gives an explicit treatment of the nonconservative product.

We begin by replacing the interfaces $x_{i+\frac{1}{2}}$ by singular layers (or internal boundary layers)

$$\widehat{C}^\varepsilon_{i+\frac{1}{2}} := [x_{i+\frac{1}{2}} - \varepsilon, x_{i+\frac{1}{2}} + \varepsilon].$$

Over each of these infinitesimal layers the bottom is reconstructed continuously by a function $z_\varepsilon(x)$. This removes the bottom singularity in the nonconservative product. The flow variables are reconstructed by piecewise continuous functions $h_\varepsilon(x)$, $w_\varepsilon(x)$, and $u_\varepsilon(x)$ over the singular subcells

$$\widehat{C}^\varepsilon_{i+\frac{1}{2}-} := [x_{i+\frac{1}{2}} - \varepsilon, x_{i+\frac{1}{2}}] \quad \text{and} \quad \widehat{C}^\varepsilon_{i+\frac{1}{2}+} := [x_{i+\frac{1}{2}}, x_{i+\frac{1}{2}} + \varepsilon].$$

These reconstructions provide the data of the Riemann problem at the interface, with an approximate Riemann solver $F_\varepsilon(x_{i+\frac{1}{2}})$. The source term is computed over the singular subcells. Together, this gives the residuum

$$(3.1) \qquad R^\varepsilon_i := -\frac{1}{\Delta x}\left(F_\varepsilon(x_{i+\frac{1}{2}}) - F_\varepsilon(x_{i-\frac{1}{2}})\right) + \frac{1}{\Delta x}\int_{C_i} S(U_\varepsilon(x), z_\varepsilon(x))dx.$$

In Theorem 3.5 we prove that

$$\lim_{\varepsilon \to 0} R_i^\varepsilon = R_i, \tag{3.2}$$

where R_i is the original residuum from (1.3).

> *Remark* 3.1.
> (i) Note that the construction procedure summarized in (3.2) has already been used in [18, 19] to define a high order well-balanced scheme for moving water. Here we use it to derive a new HR scheme, which is tailored to the wet-dry front.
> (ii) In Remark 3.6 below, we will use the subcell reconstruction to highlight a key difference between the three schemes.
> (iii) It is an interesting question under which conditions a subcell reconstruction may be interpreted as a path in the sense of [9, 20].

The details of the approximation are given in the following subsections.

3.1. Splitting the cells into subcells. Let us denote the interior subcell by $C_i^\varepsilon := \left[x_{i-\frac{1}{2}} + \varepsilon, x_{i+\frac{1}{2}} - \varepsilon \right]$. Then

$$C_i = \widehat{C}_{i-\frac{1}{2}+}^\varepsilon \cup C_i^\varepsilon \cup \widehat{C}_{i+\frac{1}{2}-}^\varepsilon. \tag{3.3}$$

The piecewise continuous reconstruction is defined as follows.

DEFINITION 3.2 (subcell reconstruction). *Given values φ_i and $\varphi_{i+\frac{1}{2}\pm}$ for $i \in \mathbf{Z}$, let $\widehat{\varphi}_{i+\frac{1}{2}\pm}^\varepsilon : \widehat{C}_{i+\frac{1}{2}\pm}^\varepsilon \to \mathbf{R}$ be Lipschitz continuous functions with boundary values*

$$\varphi_{i+\frac{1}{2}\pm}(x_{i+\frac{1}{2}}) = \varphi_{i+\frac{1}{2}\pm}, \quad \varphi_{i+\frac{1}{2}\pm}(x_{i+\frac{1}{2}} \pm \varepsilon) = \varphi_{i+(1\pm1)/2}.$$

Then $\varphi_\varepsilon : \mathbf{R} \to \mathbf{R}$ is the piecewise continuous function given by

$$\varphi_\varepsilon(x) := \begin{cases} \varphi_i & \text{if } x \in C_i^\varepsilon, \\ \widehat{\varphi}_{i+\frac{1}{2}\pm}^\varepsilon(x) & \text{if } x \in \widehat{C}_{i+\frac{1}{2}\pm}^\varepsilon. \end{cases} \tag{3.4}$$

Remark 3.3. If $\widehat{\varphi}_{i+\frac{1}{2}-}^\varepsilon$ and $\widehat{\varphi}_{i+\frac{1}{2}+}^\varepsilon$ are both linear, we call them the *standard subcell reconstruction at interface $x_{i+\frac{1}{2}}$*. The only exception from the standard subcell reconstruction will occur in the definition of the water level for Audusse's and Morales' schemes for partially wet interfaces (see (3.13) and Figure 3 below).

To distinguish the related reconstructions for the three HR schemes of Audusse, Morales, and the present paper, we will denote them by

$$\varphi_\varepsilon^{\text{AUD}}, \varphi_\varepsilon^{\text{MOR}}, \varphi_\varepsilon^{\text{CN}}. \tag{3.5}$$

3.2. Reconstruction of the bottom $z_\varepsilon(x)$. For all three HR schemes, a continuous bottom is defined by the standard subcell reconstruction (see Definition 3.2) with

$$z_{i-\frac{1}{2}+} := z_{i-\frac{1}{2}}, \quad z_{i+\frac{1}{2}-} := z_{i+\frac{1}{2}}, \tag{3.6}$$

where the values $z_{i\pm\frac{1}{2}}$ are defined in section 2 for each of the three schemes, respectively.

Note that the reconstructed bottom is globally continuous for fixed $\varepsilon > 0$, but will have steep layers in $\widehat{C}_{i+\frac{1}{2}-}^\varepsilon$ and $\widehat{C}_{i+\frac{1}{2}+}^\varepsilon$.

3.3. Infinitesimal HR. Next we reconstruct the water level and height. Several modern well-balanced schemes such as [23, 13], as well as the present HR schemes, use the fact that the water level $w(x)$ is constant for still water. Hence the piecewise constant reconstruction becomes exact for this important equilibrium state. Given the bottom topography $z_\varepsilon(x)$, these schemes reconstruct the water level $w_\varepsilon(x)$ and then simply define the reconstructed water height as

$$(3.7) \qquad h_\varepsilon(x) = w_\varepsilon(x) - z_\varepsilon(x).$$

The conservative variables are given by

$$(3.8) \qquad U_\varepsilon(x) = \begin{pmatrix} h_\varepsilon(x) \\ h_\varepsilon(x)u_i \end{pmatrix} \qquad \forall x \in C_i.$$

For the calculations of the flux and the source term in the next subsection, we give the integral averages of $h_\varepsilon(x)$ in subcells $\hat{C}^\varepsilon_{i+\frac{1}{2}-}$ and $\hat{C}^\varepsilon_{i+\frac{1}{2}+}$:

$$(3.9) \qquad \bar{h}_{i+\frac{1}{2}-} := \frac{1}{\varepsilon} \int\limits_{\hat{C}^\varepsilon_{i+\frac{1}{2}-}} h_\varepsilon(x)dx, \quad \bar{h}_{i+\frac{1}{2}+} := \frac{1}{\varepsilon} \int\limits_{\hat{C}^\varepsilon_{i+\frac{1}{2}+}} h_\varepsilon(x)dx.$$

3.3.1. The original HR method. We define $w_\varepsilon(x)$ as in Definition 3.2, with

$$(3.10) \qquad w_i^{\mathrm{AUD}} := z_i + h_i, \quad w_{i+1}^{\mathrm{AUD}} := z_{i+1} + h_{i+1},$$

$$(3.11) \qquad w_{i+\frac{1}{2}-}^{\mathrm{AUD}} := \max(z_{i+\frac{1}{2}}^{\mathrm{AUD}}, w_i), \quad w_{i+\frac{1}{2}+}^{\mathrm{AUD}} := \max(z_{i+\frac{1}{2}}^{\mathrm{AUD}}, w_{i+1}).$$

In the fully wet case (see Figure 2),

$$(3.12) \qquad \widehat{w}_{i+\frac{1}{2}-}^{\mathrm{AUD}}(x) \equiv w_i, \quad \widehat{w}_{i+\frac{1}{2}+}^{\mathrm{AUD}}(x) \equiv w_{i+1},$$

while in the partially wet case (see Figure 3),

$$(3.13) \qquad \widehat{w}_{i+\frac{1}{2}-}^{\mathrm{AUD}}(x) := \max(z_\varepsilon^{\mathrm{AUD}}(x), w_i), \quad \widehat{w}_{i+\frac{1}{2}+}^{\mathrm{AUD}}(x) := \max(z_\varepsilon^{\mathrm{AUD}}(x), w_{i+1}).$$

This is the only instance where our subcell reconstruction may differ from the standard definition. In fact, this will happen if and only if the wet-dry front is contained in one of the cells $\widehat{C}^\varepsilon_{i+\frac{1}{2}-}$ or $\widehat{C}^\varepsilon_{i+\frac{1}{2}+}$. Figure 3 displays the different subcell reconstructions for this case.

Next, we consider the average of $h_\varepsilon^{\mathrm{AUD}}(x)$ over subcells $\widehat{C}^\varepsilon_{i+\frac{1}{2}-}$ and $\widehat{C}^\varepsilon_{i+\frac{1}{2}+}$. We first consider $\widehat{C}^\varepsilon_{i+\frac{1}{2}+}$. There are two cases to be discussed.
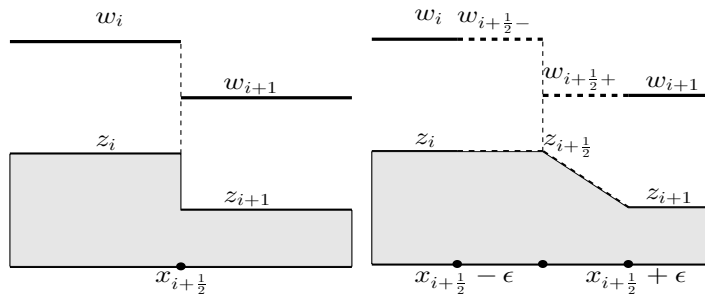

FIG. 2. *Subcell reconstruction of topography and water level for the fully wet case. Left: Riemann data. Right: reconstructed $z_\varepsilon(x)$ and $w_\varepsilon(x)$ for all three HR schemes.*
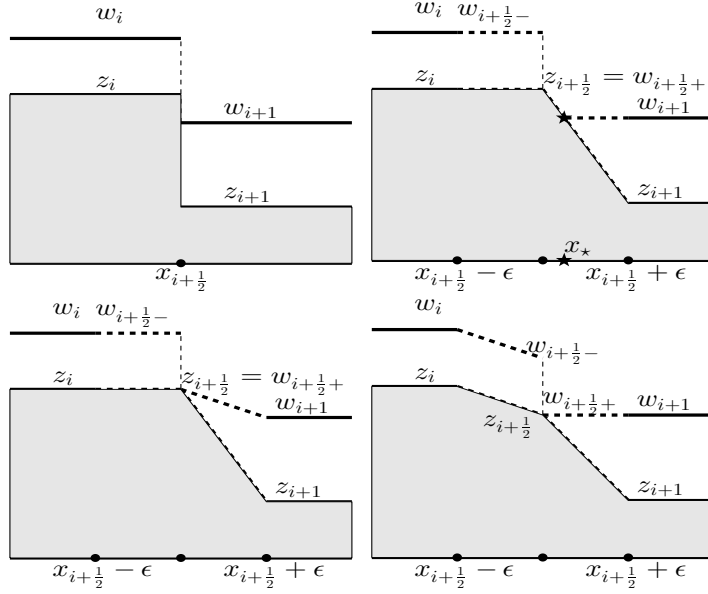
FIG. 3. *Subcell reconstruction of topography and water level for the partially wet case. Top left: Riemann data. Top right: Audusse or Morales scheme for slow uphill flow (note the vacuum region $[x_{i+\frac{1}{2}}, x_*]$). Bottom left: Morales scheme for fast uphill flow. Bottom Right: CN scheme.*

(i) In the fully wet case (in which all three schemes coincide) the water height $\widehat{h}^{\text{AUD}}_{i+\frac{1}{2}+}$ is linear, so

$$(3.14) \qquad \overline{h}^{\text{AUD}}_{i+\frac{1}{2}+} = \frac{h^{\text{AUD}}_{i+\frac{1}{2}+} + h_{i+1}}{2}.$$

(ii) In the partially wet case, $h^{\text{AUD}}_{i+\frac{1}{2}+} = 0$ (see top right of Figure 3). Assume that the wet front is located at $x_\star \in \widehat{C}^\varepsilon_{i+\frac{1}{2}+}$. Then the average water height is

$$(3.15) \qquad \overline{h}^{\text{AUD}}_{i+\frac{1}{2}+} = \frac{x_{i+\frac{1}{2}} + \varepsilon - x_\star}{\varepsilon} \frac{h(x_\star) + h_{i+1}}{2} = \frac{h_{i+1}}{z_{i+\frac{1}{2}} - z_{i+1}} \frac{h_{i+1}}{2},$$

where we have used the intercept theorem in the last equality. Summarizing (3.14) and (3.15), we obtain

$$(3.16) \qquad \overline{h}^{\text{AUD}}_{i+\frac{1}{2}+} = \begin{cases} \frac{h_{i+1} + h^{\text{AUD}}_{i+\frac{1}{2}+}}{2}, & h^{\text{AUD}}_{i+\frac{1}{2}+} > 0, \\ \frac{h_{i+1}}{2} \frac{h_{i+1}}{z^{\text{AUD}}_{i+\frac{1}{2}} - z_{i+1}}, & h^{\text{AUD}}_{i+\frac{1}{2}+} = 0. \end{cases}$$

Similarly,

$$(3.17) \qquad \overline{h}^{\text{AUD}}_{i+\frac{1}{2}-} = \begin{cases} \frac{h_i + h^{\text{AUD}}_{i+\frac{1}{2}-}}{2}, & h^{\text{AUD}}_{i+\frac{1}{2}-} > 0, \\ \frac{h_i}{2} \frac{h_i}{z^{\text{AUD}}_{i+\frac{1}{2}} - z_i}, & h^{\text{AUD}}_{i+\frac{1}{2}-} = 0. \end{cases}$$

3.3.2. The HR scheme of Morales et al. The continuous bottom of Morales' scheme coincides with that of the original HR scheme:

$$(3.18) \qquad z_\varepsilon^{\mathrm{MOR}}(x) \equiv z_\varepsilon^{\mathrm{AUD}}(x).$$

The water level coincides with that of the original scheme, except for the partially wet interfaces (2.3). If the water flows downhill, or uphill with enough kinetic energy to climb the discrete jump of the bottom, i.e., (2.11) (resp., (2.13)) holds, then over $\hat{C}_{i+\frac{1}{2}-}$ (resp., $\hat{C}_{i+\frac{1}{2}+}$) the reconstructed water level $w_\varepsilon^{\mathrm{MOR}}(x)$ is given by the standard subcell reconstruction (see Definition 3.2) instead of Audusse's piecewise linear reconstruction (3.11) (see Figure 3). Then the local averages of $h_\varepsilon^{\mathrm{MOR}}(x)$ over subcells $\widehat{C}_{i+\frac{1}{2}-}^\varepsilon$ (resp., $\hat{C}_{i+\frac{1}{2}+}^\varepsilon$) are simply

$$(3.19) \quad \bar{h}_{i+\frac{1}{2}-}^{\mathrm{MOR}} = \frac{h_i + h_{i+\frac{1}{2}-}^{\mathrm{MOR}}}{2} = \frac{h_i}{2} \quad \left(\mathrm{resp.}, \quad \bar{h}_{i+\frac{1}{2}+}^{\mathrm{MOR}} = \frac{h_{i+1} + h_{i+\frac{1}{2}+}^{\mathrm{MOR}}}{2} = \frac{h_{i+1}}{2} \right),$$

since $h_{i+\frac{1}{2}-}^{\mathrm{MOR}} = 0$ $\left(\mathrm{resp.}, h_{i+\frac{1}{2}+}^{\mathrm{MOR}} = 0 \right)$.

3.3.3. The present HR scheme. The continuous bottom of our new scheme, $z_\varepsilon^{\mathrm{CN}}$, is defined by the standard subcell reconstruction with

$$(3.20) \qquad z_{i+\frac{1}{2}-}^{\mathrm{CN}} = z_{i+\frac{1}{2}+}^{\mathrm{CN}} = z_{i+\frac{1}{2}}^{\mathrm{CN}}$$

(see (2.15) for the pointvalues $z_{i+\frac{1}{2}}^{\mathrm{CN}}$). The reference values for the water surface are given by

$$(3.21) \qquad w_{i+\frac{1}{2}-}^{\mathrm{CN}} := \min(w_i, z_{i+\frac{1}{2}}^{\mathrm{CN}} + h_i), \quad w_{i+\frac{1}{2}+}^{\mathrm{CN}} := \min(w_{i+1}, z_{i+\frac{1}{2}}^{\mathrm{CN}} + h_{i+1}),$$

and the reference values for the water depth are given by (2.16). Due to the linearity of $\widehat{h}_{i+\frac{1}{2}-}$ (resp., $\widehat{h}_{i+\frac{1}{2}+}$), the average values of h_ε over the singular subcells $\widehat{C}_{i+\frac{1}{2}-}^\varepsilon$ (resp., $\widehat{C}_{i+\frac{1}{2}+}^\varepsilon$) are

$$(3.22) \qquad \bar{h}_{i+\frac{1}{2}-}^{\mathrm{CN}} = \frac{h_i + h_{i+\frac{1}{2}-}^{\mathrm{CN}}}{2}, \quad \left(\mathrm{resp.}, \quad \bar{h}_{i+\frac{1}{2}+}^{\mathrm{CN}} = \frac{h_{i+1} + h_{i+\frac{1}{2}+}^{\mathrm{CN}}}{2} \right).$$

Remark 3.4. From (3.16), (3.17) ,(3.19) and (3.22), the subcell averages $\bar{h}_{i+\frac{1}{2}-}$ and $\bar{h}_{i+\frac{1}{2}+}$ of $h_\varepsilon(x)$ over subcells $\widehat{C}_{i+\frac{1}{2}-}^\varepsilon$ and $\widehat{C}_{i+\frac{1}{2}+}^\varepsilon$ obtained by the three schemes are in fact independent of ε.

3.4. Fluxes and source terms based on subcell reconstructions. For all three hydrostatic schemes the flux vector $F_\varepsilon(x)$ is reconstructed by the standard subcell reconstruction (see Definition 3.2) with reference values

$$(3.23) \qquad F_i := F(U_i), \quad F_{i+\frac{1}{2}-} := F_{i+\frac{1}{2}+} := F_{i+\frac{1}{2}},$$

where

$$(3.24) \qquad F_{i+\frac{1}{2}} := \mathcal{F}\left(U_{i+\frac{1}{2}-}, U_{i+\frac{1}{2}+} \right)$$

is an approximate Riemann solver as defined in section 2.4. Note that $F_\varepsilon(x)$ is globally continuous. The definition of the reconstructed source term $S_\varepsilon(x) := \left(0, s_\varepsilon(x)\right)^T$ takes the natural form

(3.25) $$s_\varepsilon(x) := -g\, h_\varepsilon(x)\, \partial_x z_\varepsilon(x)$$

and hence corresponds directly to (1.4).

Given (3.23)–(3.25), we now introduce the reconstructed, cell-averaged residuum by

(3.26) $$R_i^\varepsilon := -\frac{1}{\Delta x}\big(F_\varepsilon(x_{i+\frac{1}{2}}) - F_\varepsilon(x_{i-\frac{1}{2}})\big) + \frac{1}{\Delta x}\int_{C_i} S(U_\varepsilon(x), z_\varepsilon(x))dx.$$

Depending on the choice of hydrostatic scheme, we denote the residuums by $R_i^{\varepsilon,\mathrm{AUD}}$, $R_i^{\varepsilon,\mathrm{MOR}}$, and $R_i^{\varepsilon,\mathrm{CN}}$. The key result of this section is the following theorem.

THEOREM 3.5. *For each of the three hydrostatic schemes, and for each cell C_i, the reconstructed residuums are independent of ε, $R_i^\varepsilon = \overline{R}_i$ for all $\varepsilon > 0$, and coincide with the original definitions given in section 2:*

(3.27) $$\overline{R}_i^{\,\mathrm{AUD}} = R_i^{\,\mathrm{AUD}}, \quad \overline{R}_i^{\,\mathrm{MOR}} = R_i^{\,\mathrm{MOR}}, \quad \overline{R}_i^{\,\mathrm{CN}} = R_i^{\,\mathrm{CN}}.$$

Proof. Since the flux differences in (1.3) and (3.1) coincide,

(3.28) $$\lim_{\varepsilon\to 0} R_i^\varepsilon - R_i = \left(\lim_{\varepsilon\to 0}\frac{1}{\Delta x}\int_{C_i} S(U_\varepsilon(x), z_\varepsilon(x))dx\right) - S_i = \left(0,\ \lim_{\varepsilon\to 0} s_i^\varepsilon - s_i\right)^T,$$

where $s_i^\varepsilon := \frac{-g}{\Delta x}\int_{C_i} h_\varepsilon(x)\partial_x z_\varepsilon(x)dx$. By the linearity of $z_\varepsilon(x)$,

$$s_i^\varepsilon = -\frac{g}{\Delta x}\int_{\hat{C}^\varepsilon_{i-\frac{1}{2}+}} h_\varepsilon(x)\partial_x z_\varepsilon(x)dx - \frac{g}{\Delta x}\int_{\hat{C}^\varepsilon_{i+\frac{1}{2}-}} h_\varepsilon(x)\partial_x z_\varepsilon(x)dx$$

$$= -\frac{g}{\Delta x}\frac{z_i - z_{i-\frac{1}{2}}}{\varepsilon}\int_{\hat{C}^\varepsilon_{i-\frac{1}{2}+}} h_\varepsilon(x)dx - \frac{g}{\Delta x}\frac{z_{i+\frac{1}{2}} - z_i}{\varepsilon}\int_{\hat{C}^\varepsilon_{i+\frac{1}{2}-}} h_\varepsilon(x)dx$$

(3.29) $$= -\frac{g}{\Delta x}\bar{h}_{i-\frac{1}{2}+}(z_i - z_{i-\frac{1}{2}}) - \frac{g}{\Delta x}\bar{h}_{i+\frac{1}{2}-}(z_{i+\frac{1}{2}} - z_i),$$

which is independent of ε due to Remark 3.4. It remains to show that for all three HR schemes,

(3.30) $$\lim_{\varepsilon\to 0} s_i^\varepsilon - s_i = 0.$$

(i) *Audusse's scheme.* First we show that the first term on the right-hand side of (3.29) equals the left source term in the original HR scheme, as defined in (2.8), i.e., we prove that

(3.31) $$-\frac{g}{\Delta x}\bar{h}_{i-\frac{1}{2}+}^{\mathrm{AUD}}(z_i - z_{i-\frac{1}{2}}^{\mathrm{AUD}}) = \frac{g}{2\Delta x}((h_i)^2 - (h_{i-\frac{1}{2}+}^{\mathrm{AUD}})^2).$$

First suppose that $z_{i-\frac{1}{2}}^{\mathrm{AUD}} = z_i$. From (2.6),

$$h_{i-\frac{1}{2}+}^{\mathrm{AUD}} = \max(w_i - z_{i-\frac{1}{2}}^{\mathrm{AUD}}, 0) = \max(z_i + h_i - z_i, 0) = h_i.$$

Therefore, both sides of (3.31) vanish in this case. Next, suppose that $z_{i-\frac{1}{2}}^{\mathrm{AUD}} = z_{i-1}$. Again, from (2.6),

$$h_{i-\frac{1}{2}+}^{\mathrm{AUD}} = \max(w_i - z_{i-\frac{1}{2}}^{\mathrm{AUD}}, 0) = \max(z_i + h_i - z_{i-1}, 0).$$

If $h_{i-\frac{1}{2}+}^{\mathrm{AUD}} > 0$, then

$$-\frac{g}{\Delta x}\bar{h}_{i-\frac{1}{2}+}^{\mathrm{AUD}}(z_i - z_{i-\frac{1}{2}}^{\mathrm{AUD}}) = -\frac{g}{2\Delta x}(h_i + h_{i-\frac{1}{2}+}^{\mathrm{AUD}})(z_i - z_{i-1})$$

(3.32)
$$= -\frac{g}{2\Delta x}(h_i + h_{i-\frac{1}{2}+}^{\mathrm{AUD}})(h_{i-\frac{1}{2}+}^{\mathrm{AUD}} - h_i),$$

which is the right-hand side of (3.31). If $h_{i-\frac{1}{2}+}^{\mathrm{AUD}} = 0$, then by (3.17),

(3.33) $$-\frac{g}{\Delta x}\bar{h}_{i-\frac{1}{2}+}^{\mathrm{AUD}}(z_i - z_{i-\frac{1}{2}}^{\mathrm{AUD}}) = -\frac{g}{\Delta x}\frac{h_i}{2}\frac{h_i}{z_{i-1} - z_i}(z_i - z_{i-1}) = \frac{g(h_i)^2}{2\Delta x},$$

which again coincides with the right-hand side of (3.31). The second term on the right-hand side of (3.29) can be treated analogously. This proves the theorem for Audusse's scheme.

(ii) *The HR scheme of Morales et al.* This scheme differs from the original HR scheme only when the water flows up a partially wet bottom. From (3.19) and (2.12), one can see immediately that

(3.34) $$-\frac{g}{\Delta x}\bar{h}_{i-\frac{1}{2}+}^{\mathrm{MOR}}(z_i - z_{i-\frac{1}{2}}^{\mathrm{MOR}}) = -\frac{g}{\Delta x}\frac{h_i}{2}(z_i - z_{i-\frac{1}{2}}^{\mathrm{MOR}}) = s_{i+\frac{1}{2}-}^{\mathrm{MOR}}.$$

Similarly, one can see from (3.19) and (2.14) that

(3.35) $$-\frac{g}{\Delta x}\bar{h}_{i+\frac{1}{2}-}^{\mathrm{MOR}}(z_{i+\frac{1}{2}}^{\mathrm{MOR}} - z_i) = -\frac{g}{\Delta x}\frac{h_i}{2}(z_i - z_{i-\frac{1}{2}}^{\mathrm{MOR}}) = s_{i-\frac{1}{2}+}^{\mathrm{MOR}}.$$

This finishes the proof of the theorem for Morales' scheme.

(iii) *The present HR scheme.* Using (3.22), we have

$$-\frac{g}{\Delta x}\bar{h}_{i-\frac{1}{2}+}^{\mathrm{CN}}(z_i - z_{i-\frac{1}{2}}^{\mathrm{CN}}) = -\frac{g}{\Delta x}\frac{h_i + h_{i-\frac{1}{2}+}^{\mathrm{CN}}}{2}(z_i - z_{i-\frac{1}{2}}^{\mathrm{CN}}) = s_{i-\frac{1}{2}+}^{\mathrm{CN}},$$

$$-\frac{g}{\Delta x}\bar{h}_{i+\frac{1}{2}-}^{\mathrm{CN}}(z_{i+\frac{1}{2}}^{\mathrm{CN}} - z_i) = -\frac{g}{\Delta x}\frac{h_i + h_{i+\frac{1}{2}-}^{\mathrm{CN}}}{2}(z_{i+\frac{1}{2}}^{\mathrm{CN}} - z_i) = s_{i-\frac{1}{2}+}^{\mathrm{CN}}.$$

This concludes the proof for the present scheme, and hence of Theorem 3.5.   □

Remark 3.6.
 (i) The subcell reconstructions offer a systematic approach to constructing both known and new HR schemes.
(ii) The main advantage of the present scheme is its accuracy for shallow downhill flows. This can already be predicted from Figure 3: Consider the bottom slope from z_i on the left to the water level w_{i+1} on the right. Does it contribute to an acceleration of the flow to the right? For Audusse's scheme it does not, since the water height $h_\varepsilon(x)$ in the subcell reconstruction is zero. For the present scheme, however, the water height over this piece of downhill slope is $h_\varepsilon(x) \equiv h_i$, so
$$s_{i+\frac{1}{2}-}^{\mathrm{CN}} = -\frac{g}{\Delta x}h_i(w_i - z_i).$$
This will be highlighted in the numerical experiments in section 5.

3.5. Comparison of the HR schemes. We conclude this section with a detailed comparison of the three HR schemes. In Proposition 3.7, we show that the current HR scheme only differs from the previous methods in the partially wet case (2.3). Moreover, it differs only in $\overline{h}_{i+\frac{1}{2}\pm}$ and $z_{i+\frac{1}{2}}$.

PROPOSITION 3.7.
 (i) *For all interfaces* $x_{i+\frac{1}{2}}$,

$$(3.36) \qquad\qquad h^{AUD}_{i+\frac{1}{2}\pm} = h^{MOR}_{i+\frac{1}{2}\pm} = h^{CN}_{i+\frac{1}{2}\pm}$$

and

$$(3.37) \qquad\qquad 0 \le h_{i+\frac{1}{2}-} \le h_i, \qquad 0 \le h_{i+\frac{1}{2}+} \le h_{i+1}.$$

 (ii) *For fully wet interfaces* $x_{i+\frac{1}{2}}$ *(see (2.2)),*

$$(3.38) \qquad z^{AUD}_{i+\frac{1}{2}} = z^{MOR}_{i+\frac{1}{2}} = z^{CN}_{i+\frac{1}{2}} \quad \text{and} \quad \overline{h}^{AUD}_{i+\frac{1}{2}\pm} = \overline{h}^{MOR}_{i+\frac{1}{2}\pm} = \overline{h}^{CN}_{i+\frac{1}{2}\pm}.$$

 (iii) *For partially wet interfaces* $x_{i+\frac{1}{2}}$ *(see (2.3)), and if water flows downhill, or if it flows uphill with too little kinetic energy to climb the discrete jump of the bottom (i.e., neither (2.11) nor (2.13) holds), then*

$$(3.39) \qquad z^{AUD}_{i+\frac{1}{2}} = z^{MOR}_{i+\frac{1}{2}} \qquad \text{and} \qquad \overline{h}^{AUD}_{i+\frac{1}{2}\pm} = \overline{h}^{MOR}_{i+\frac{1}{2}\pm}.$$

Proof. The proof is a direct computation based on the definition of the interface values (2.5), (2.6), (2.15), and (2.16), and the integral averages of the subcell water heights defined in (3.9). □

4. Stability analysis. The present section establishes the stability of the new HR scheme. In Theorem 4.1, we prove positivity of the water height. In Theorem 4.3, we show that the scheme is well balanced for the lake at rest. In Theorem 4.6, we establish a semidiscrete entropy inequality. The proofs are closely related to those in [2]. Note that we omit the superscript CN when there is no confusion.

To simplify the proofs, we use the well-known convex decomposition of the semidiscrete finite volume scheme (1.3):

$$\frac{d}{dt}U_i(t) = R_{i-\frac{1}{2}+} + R_{i+\frac{1}{2}-}$$
$$(4.1) \qquad := -\frac{1}{\Delta x}\big(F(U_i) - F_{i-\frac{1}{2}}\big) + S_{i-\frac{1}{2}+} - \frac{1}{\Delta x}\big(F_{i+\frac{1}{2}} - F(U_i)\big) + S_{i+\frac{1}{2}-}.$$

The first theorem states that our scheme preserves the positivity of the water height under the same condition as Audusse's scheme.

THEOREM 4.1 (positivity). *Under condition (2.21), the new semidiscrete HR scheme guarantees nonnegative water height for the homogeneous shallow water equations.*

Proof. Suppose that the ith cell is empty, $h_i = 0$. We need to prove that

$$R^{(h)}_{i-\frac{1}{2}+} \ge 0 \quad \text{and} \quad R^{(h)}_{i+\frac{1}{2}-} \ge 0,$$

where, as before, the superscript (h) denotes the first component of a vector. Let us start with the residuum over the left subcell: from (3.37) it follows that $h_{i-\frac{1}{2}+} = 0$, and hence (2.4) implies that $U_{i-\frac{1}{2}+} = \mathbf{0}$. Therefore,

$$R^{(h)}_{i-\frac{1}{2}+} = -\frac{1}{\Delta x}\left(F(U_i)^{(h)} - F^{(h)}_{i-\frac{1}{2}}\right) = \frac{1}{\Delta x}\mathcal{F}(U_{i-\frac{1}{2}-}, \mathbf{0})^{(h)}.$$

Due to condition (2.21) this is nonnegative. The proof for the right subcell is analogous. □

Before we establish that our scheme is well-balanced, we would like to distinguish the following two classes of equilibria.

DEFINITION 4.2.
(i) *Given a constant water level w_{eq}, the* still water equilibrium *is given by $u(x) \equiv 0$ and*

(4.2) $$h(x) + z(x) \equiv w_{eq}.$$

The cell averages are consistent with the still water equilibrium, if for all i, $u_i = 0$ and

(4.3) $$h_i + z_i = w_{eq}.$$

(ii) *The* lake at rest equilibrium *is given by $u(x) \equiv 0$ and*

(4.4) $$h(x)\, \partial_x(h(x) + z(x)) \equiv 0$$

for some constant $w_{eq} \geq \max\limits_{x \in \mathbf{R}} z(x)$. Moreover, near a wet-dry interface, the dry part of z should not be lower than the adjacent water level.
   The cell averages are locally *(at interface $x_{i+\frac{1}{2}}$) consistent with the lake at rest, if $u_i = u_{i+1} = 0$ and either $x_{i+\frac{1}{2}}$ is an interior interface (the still water case)*

(4.5) $$h_i > 0, \quad h_{i+1} > 0, \quad and \quad h_i + z_i = h_{i+1} + z_{i+1},$$

or a dry-wet front

(4.6) $$h_i = 0, \quad h_{i+1} > 0, \quad and \quad z_i \geq h_{i+1} + z_{i+1},$$

or a wet-dry front

(4.7) $$h_i > 0, \; h_{i+1} = 0, \quad and \quad z_{i+1} \geq h_i + z_i,$$

or dry

(4.8) $$h_i = h_{i+1} = 0.$$

The cell averages are globally consistent with the lake at rest, *if they are locally consistent with the lake at rest for all interfaces $x_{i+\frac{1}{2}}$.*
(iii) *Suppose that the cell averages of the semidiscrete finite volume scheme (1.3) are consistent with a given equilibrium state. Then we call the scheme* well balanced *for this equilibrium state if $R_i = 0$ for all i.*

THEOREM 4.3 (well-balancing). *The present HR scheme is well balanced for the lake at rest.*

Proof. By inspection, $R^{(h)}_{i+\frac{1}{2}-} = R^{(h)}_{i-\frac{1}{2}+} = 0$ for all interfaces. It remains to show that $R^{(hu)}_{i+\frac{1}{2}-} = R^{(hu)}_{i-\frac{1}{2}+} = 0$ as well.

(i) We begin with the interior interface (4.5). Here the flow is locally in still water equilibrium, and the interface $x_{i+\frac{1}{2}}$ is fully wet in the sense of (2.2). Therefore, our new scheme coincides with that of Audusse et al., and

$$R_{i+\frac{1}{2}-}^{(hu)} = \left(R_{i+\frac{1}{2}-}^{\text{AUD}}\right)^{(hu)} = 0.$$

(ii) Next, let us consider a dry-wet front as in (4.6). By (3.37), $h_{i+\frac{1}{2}-} = 0$. Thus from (3.22), $\overline{h}_{i+\frac{1}{2}-} = 0$. From (2.15) and (4.6),

$$z_{i+\frac{1}{2}} = \min\left(\max(z_i, z_{i+1}), \min(w_i, w_{i+1})\right) = \min\left(z_i, w_{i+1}\right) = w_{i+1}.$$

From this and (2.16), $h_{i+\frac{1}{2}+} = 0$ as well. Therefore, $U_{i+\frac{1}{2}-} = U_{i+\frac{1}{2}+} = \mathbf{0}$, and by consistency of the approximate Riemann solver, $F_{i+\frac{1}{2}} = \mathcal{F}(\mathbf{0}, \mathbf{0}) = \mathbf{0}$. The source term vanishes as well: $s_{i+\frac{1}{2}-} = -\frac{g}{\Delta x}\overline{h}_{i+\frac{1}{2}-}(z_{i+\frac{1}{2}} - z_i) = 0$. Therefore, $R_{i+\frac{1}{2}-}^{(hu)} = 0$.

Now we show that $R_{i+\frac{1}{2}+}^{(hu)} = 0$. Note that

$$F(U_{i+1})^{(hu)} = \frac{g}{2}h_{i+1}^2, \qquad \overline{h}_{i+\frac{1}{2}+} = \frac{h_{i+\frac{1}{2}+} + h_{i+1}}{2} = \frac{h_{i+1}}{2},$$

and

$$s_{i+\frac{1}{2}+} = -\frac{g}{\Delta x}\overline{h}_{i+\frac{1}{2}+}(z_{i+1} - z_{i+\frac{1}{2}}) = -\frac{g}{\Delta x}\frac{h_{i+1}}{2}(z_{i+1} - (z_{i+1} + h_{i+1}))$$
$$= \frac{g}{\Delta x}\frac{h_{i+1}^2}{2}.$$

Therefore,

$$R_{i+\frac{1}{2}+}^{(hu)} = -\frac{1}{\Delta x}(F(U_{i+1})^{(hu)} - F_{i+\frac{1}{2}}^{(hu)}) + s_{i+\frac{1}{2}+} = -\frac{1}{\Delta x}F(U_{i+1})^{(hu)} + s_{i+\frac{1}{2}+} = 0.$$

(iii) The wet-dry case (4.7) can be treated analogously, and the dry case follows by inspection.   □

The remainder of this section is devoted to proving a semidiscrete entropy inequality for the new HR scheme. It is well known (see, e.g., [6]) that the shallow water equations with bottom source term (1.1) admit the following entropy inequality, related to the physical energy:

$$\partial_t \tilde{\eta}(U, z) + \partial_x \tilde{G}(U, z) \leq 0.$$

Here $\tilde{\eta}(U, z) := \eta(U, z) + ghz$ and $\tilde{G}(U, z) := G(U, z) + ghuz$ are the entropy and entropy-flux, respectively, which in turn are based on the entropy and entropy-flux for the homogeneous shallow water equations, $\eta(U) := \frac{1}{2}hu^2 + \frac{1}{2}gh^2$ and $G(U) := (\frac{1}{2}hu^2 + gh^2)u$. It is useful to write down the Jacobian of $\eta(U)$ and $\tilde{\eta}(U, z)$ with respect to U:

(4.9) $\eta'(U) = \begin{pmatrix} gh - \frac{u^2}{2} \\ u \end{pmatrix}, \quad \tilde{\eta}'(U, z) = \eta'(U) + \begin{pmatrix} gz \\ 0 \end{pmatrix}.$

Let us recall the classical semidiscrete entropy inequality.

DEFINITION 4.4. *A semidiscrete scheme for the homogeneous problem*

$$\Delta x_i \frac{dU_i(t)}{dt} + \mathcal{F}(U_i, U_{i+1}) - \mathcal{F}(U_{i-1}, U_i) = 0 \tag{4.10}$$

with numerical flux $\mathcal{F}$ consistent with $F(U)$ satisfies the in-cell entropy inequality, if there exists a numerical entropy flux $\mathcal{G}$ consistent with $G(U)$ such that

$$\Delta x_i \frac{d\eta(U_i(t))}{dt} + \mathcal{G}(U_i, U_{i+1}) - \mathcal{G}(U_{i-1}, U_i) \le 0. \tag{4.11}$$

Before we prove a semidiscrete entropy inequality for the new HR scheme, we summarize some important results from [2, 6]. One can refine (4.11) by dividing each cell into two subcells. In [6, Lemma 4.6] it is proved that (4.11) holds if and only if a corresponding entropy inequality holds to the left and right of each interface:

$$G(U_i) + \eta'(U_i)(\mathcal{F}(U_i, U_{i+1}) - F(U_i)) \ge \mathcal{G}(U_i, U_{i+1}) \tag{4.12}$$

$$\ge G(U_{i+1}) + \eta'(U_{i+1})(\mathcal{F}(U_i, U_{i+1}) - F(U_{i+1})). \tag{4.13}$$

To treat their HR scheme for the shallow water equations with source term, we use the shortcuts

$$F_{i+\frac{1}{2}} := \mathcal{F}(U_{i+\frac{1}{2}-}, U_{i+\frac{1}{2}+}) \quad \text{and} \quad G_{i+\frac{1}{2}} := \mathcal{G}(U_i, U_{i+1}, z_i, z_{i+1}).$$

In [2, 6], a numerical entropy flux $\tilde{G}$ for the inhomogeneous shallow water equations is introduced via

$$\tilde{G}_{i+\frac{1}{2}} := G_{i+\frac{1}{2}} + g F^h_{i+\frac{1}{2}} z_{i+\frac{1}{2}}.$$

The following lemma is at the heart of the matter.

LEMMA 4.5 (see [2, 6]).   *The semidiscrete finite volume scheme* (1.3) *satisfies the semidiscrete entropy inequality*

$$\Delta x_i \frac{d}{dt} \tilde{\eta}(U_i(t), z_i) + \tilde{G}_{i+\frac{1}{2}} - \tilde{G}_{i-\frac{1}{2}} \le 0 \tag{4.14}$$

if and only if

$$\tilde{G}(U_i, z_i) + \tilde{\eta}'(U_i, z_i)(F_{i+\frac{1}{2}} - \Delta x S_{i+\frac{1}{2}-} - F(U_i)) \ge \tilde{G}_{i+\frac{1}{2}} \tag{4.15}$$

$$\ge \tilde{G}(U_{i+1}, z_{i+1}) + \tilde{\eta}'(U_{i+1}, z_{i+1})(F_{i+\frac{1}{2}} + \Delta x S_{i+\frac{1}{2}+} - F(U_{i+1})). \tag{4.16}$$

Using this lemma, we now prove a semidiscrete entropy inequality for our new HR scheme.

THEOREM 4.6 (entropy condition).   *Assume that the semidiscrete finite-volume scheme* (4.10) *for the homogeneous shallow water equation satisfies the in-cell entropy inequality* (4.11) *and that the numerical mass flux at the wet-dry front satisfies the vacuum influx condition* (2.22). *Then the semidiscrete HR scheme* (1.3) *satisfies the entropy inequality* (4.14) *for the inhomogeneous shallow water equation.*

Proof. According to Lemma 4.5, we need to prove the two inequalities (4.15)–(4.16) for the new HR scheme. Due to symmetry, we focus on (4.15). Subtracting the two sides, we introduce the entropy production term

$$\tilde{E}_{i+\frac{1}{2}-} := \tilde{\eta}'(U_i, z_i)(-F_{i+\frac{1}{2}} + F(U_i) + \Delta x S_{i+\frac{1}{2}-}) + \tilde{G}_{i+\frac{1}{2}} - \tilde{G}(U_i, z_i).$$

Our goal is to show that $\tilde{E}_{i+\frac{1}{2}-} \leq 0$. Using (4.9) and

$$\Delta x S_{i+\frac{1}{2}-} = \left(0, -g\bar{h}_{i+\frac{1}{2}-}(z_{i+\frac{1}{2}} - z_i)\right)^T,$$

we compute

$$
\begin{aligned}
\tilde{E}&_{i+\frac{1}{2}-} \\
&= \tilde{\eta}'(U_i, z_i)(-F_{i+\frac{1}{2}} + F(U_i)) - u_i g\bar{h}_{i+\frac{1}{2}-}(z_{i+\frac{1}{2}} - z_i) \\
&\quad + G_{i+\frac{1}{2}} + gF^h_{i+\frac{1}{2}-}z_{i+\frac{1}{2}} - G(U_i) - gh_i u_i z_i \\
&= \eta'(U_i)(-F_{i+\frac{1}{2}} + F(U_i)) + G_{i+\frac{1}{2}} - G(U_i) \\
&\quad + gz_i(-F^h_{i+\frac{1}{2}} + h_i u_i) + g\left(F^h_{i+\frac{1}{2}-} - \bar{h}_{i+\frac{1}{2}-}u_i\right)z_{i+\frac{1}{2}} - g\left(h_i u_i - \bar{h}_{i+\frac{1}{2}-}u_i\right)z_i \\
&= \eta'(U_i)(-F_{i+\frac{1}{2}} + F(U_i)) + G_{i+\frac{1}{2}} - G(U_i)
\end{aligned}
$$
$$(4.17) \qquad + g\left(F^h_{i+\frac{1}{2}-} - \bar{h}_{i+\frac{1}{2}-}u_i\right)(z_{i+\frac{1}{2}} - z_i).$$

Now we evaluate (4.12) at $(U_{i+\frac{1}{2}-}, U_{i+\frac{1}{2}+})$ instead of (U_i, U_{i+1}),

$$G_{i+\frac{1}{2}} \leq \eta'(U_{i+\frac{1}{2}-})\left(F_{i+\frac{1}{2}} - F(U_{i+\frac{1}{2}-})\right) + G(U_{i+\frac{1}{2}-}),$$

and insert this into (4.17) to obtain

$$
\begin{aligned}
\tilde{E}_{i+\frac{1}{2}-} &\leq \eta'(U_i)(-F_{i+\frac{1}{2}} + F(U_i)) - G(U_i) + g\left(F^h_{i+\frac{1}{2}-} - \bar{h}_{i+\frac{1}{2}-}u_i\right)(z_{i+\frac{1}{2}} - z_i) \\
&\quad + \left(\eta'(U_{i+\frac{1}{2}-})\left(F_{i+\frac{1}{2}} - F(U_{i+\frac{1}{2}-})\right) + G(U_{i+\frac{1}{2}-})\right) \\
&=: \tilde{E}^A_{i+\frac{1}{2}-}.
\end{aligned}
$$

Using the identities

$$
\begin{aligned}
G(U) - \eta'(U)F(U) &= \left(\frac{1}{2}hu^2 + gh^2\right)u - \left(\left(gh - \frac{u^2}{2}\right)hu + u\left(hu^2 + \frac{1}{2}gh^2\right)\right) \\
&= -\frac{1}{2}gh^2 u
\end{aligned}
$$

and

$$\eta'(U_i) - \eta'(U_{i+\frac{1}{2}-}) = \begin{pmatrix} gh_i - \frac{(u_i)^2}{2} \\ u_i \end{pmatrix} - \begin{pmatrix} gh_{i+\frac{1}{2}-} - \frac{(u_i)^2}{2} \\ u_i \end{pmatrix} = \begin{pmatrix} g(h_i - h_{i+\frac{1}{2}-}) \\ 0 \end{pmatrix},$$

we calculate

$$
\begin{aligned}
\tilde{E}^A&_{i+\frac{1}{2}-} \\
&= \frac{1}{2}g((h_i)^2 - (h_{i+\frac{1}{2}-})^2)u_i - g(h_i - h_{i+\frac{1}{2}-})F^h_{i+\frac{1}{2}} + g(F^h_{i+\frac{1}{2}} - u_i\bar{h}_{i+\frac{1}{2}-})(z_{i+\frac{1}{2}} - z_i) \\
&= g\left(F^h_{i+\frac{1}{2}} - \frac{h_{i+\frac{1}{2}-} + h_i}{2}u_i\right)(h_{i+\frac{1}{2}-} - h_i) + g(F^h_{i+\frac{1}{2}} - \bar{h}_{i+\frac{1}{2}-}u_i)(z_{i+\frac{1}{2}} - z_i).
\end{aligned}
$$

For the present scheme, according to (3.14), (3.20), and (3.22), we have

$$\overline{h}_{i+\frac{1}{2}-} = \frac{h_i + h_{i+\frac{1}{2}-}}{2},$$

then $E^A_{i+\frac{1}{2}-}$ becomes

$$\tilde{E}^A_{i+\frac{1}{2}-} = g\big(F^h_{i+\frac{1}{2}} - \overline{h}_{i+\frac{1}{2}-}u_i\big)\big((h_{i+\frac{1}{2}-} + z_{i+\frac{1}{2}}) - (h_i + z_i)\big)$$

Our goal is to show that $\tilde{E}^A_{i+\frac{1}{2}-} \leq 0$. There are two cases to be discussed.

(i) In the fully wet case (see (2.2)), $\min(w_i, w_{i+1}) > \max(z_i, z_{i+1})$. According to (2.15) and (3.22), we have

$$z_{i+\frac{1}{2}} + h_{i+\frac{1}{2}-} = h_i + z_i,$$

and therefore $\tilde{E}^A_{i+\frac{1}{2}-} = 0$.

(ii) In the partially wet case (see (2.3)), $\min(w_i, w_{i+1}) \leq \max(z_i, z_{i+1})$. There are two subcases depending on whether the left bottom is higher than the right bottom.

We first consider $z_i > z_{i+1}$. According to (3.7), (3.20), (3.21), and (3.22),

(4.18) $\qquad z_{i+\frac{1}{2}} = w_{i+1}, \;\; h_{i+\frac{1}{2}-} = h_i, \;\; h_{i+\frac{1}{2}+} = 0, \;\; \text{and} \;\; \overline{h}_{i+\frac{1}{2}-} = h_i.$

Therefore,

$$\tilde{E}^A_{i+\frac{1}{2}-} = g(\mathcal{F}(h_i, h_iu_i, 0, 0) - h_iu_i)(w_{i+1} - z_i).$$

By (2.3), $w_{i+1} - z_i < 0$, and due to (2.22), $\mathcal{F}(h_i, h_iu_i, 0, 0) - h_iu_i \geq 0$. This implies that $\tilde{E}_{i+\frac{1}{2}-} \leq 0$.

Next we consider the case $z_i < z_{i+1}$. Analogously to (4.18),

$$z_{i+\frac{1}{2}} = w_i, \;\; h_{i+\frac{1}{2}-} = 0, \;\; h_{i+\frac{1}{2}+} = h_{i+1}, \;\; \text{and} \;\; \overline{h}_{i+\frac{1}{2}-} = \frac{1}{2}h_i.$$

Therefore,

$$z_{i+\frac{1}{2}} + h_{i+\frac{1}{2}-} = h_i + z_i,$$

and hence $\tilde{E}^A_{i+\frac{1}{2}-} = 0$. $\qquad\qquad\qquad\qquad\qquad\qquad\qquad\qquad\qquad\qquad\square$

5. Numerical experiments. In this section, we present several numerical experiments to test the new HR scheme. After verifying that all three schemes preserve the lake at rest (section 5.2), we study three cases of downhill flow which clearly show the advantages of the new HR scheme. The first case (section 5.3) is a thin layer of water running down a linear slope. We give an analysis of a prototype situation which clearly explains the differences between the three schemes. The second case (section 5.4) is flow over a step. The third case is a vacuum Riemann problem over a constant bottom, followed by a downward step (section 5.5). The test in section 5.6 shows an upward flow. As expected, our scheme performs comparably to the other HR schemes.

We discretize the semidiscrete finite volume scheme (1.3) in time using the forward Euler method. This yields

$$U_i^{n+1} = U_i^n + \Delta t R_i^n.$$

The time step is restricted by the CFL condition

$$\frac{\Delta t}{\Delta x} \max_i(|u_i| + a_i) < \frac{1}{2}$$

with $a_i = \sqrt{gh_i}$. The HLL flux (2.19) is used in the implementation.

5.1. Reference solutions for discontinuous topography. When the bottom is continuous, we compute the reference solution by Audusse's scheme on 10^4 uniform cells. However, in sections 5.4–5.6 the topographies are discontinuous. In this situation, the Riemann problem does not have a unique solution. To compare the three HR schemes, we need a reference solution. Ideally this reference solution should not be affected by the nonuniqueness due to the nonconservative product (1.4). An important result in this direction is due to Audusse et al. [2], who derive a semidiscrete entropy condition for the HR method if the bottom jump is of the order of the mesh size Δx. It is to be expected that this solution is unique. Motivated by this, we replace the jump by a continuous transition of width δ and then resolve the transition layer with a sufficiently fine grid (usually 100 cells). For instance, if there is a jump of $z(x)$ at x^*, with left and right bottom elevations

$$z_l := \lim_{x \to x^*-} z(x) \neq \lim_{x \to x^*+} z(x) =: z_r,$$

then we choose

(5.1)
$$z_\delta(x) := \begin{cases} z_l & \text{for } x < x^*, \\ z_l + \frac{x-x^*}{\delta}(z_r - z_l) & \text{for } x^* \leq x < x^* + \delta, \\ z_r & \text{otherwise.} \end{cases}$$

Usually we choose $\Delta x = 10^{-2}\,\delta$, so that there are 100 computational cells within the transition layer. On this grid, we solve the shallow water equations using Audusse's scheme.

5.2. Still water flow over a complex bottom. First we validate numerically that the new scheme preserves the lake at rest (including dry areas according to Definition 4.2). The bottom topography is given by

$$z(x) = \begin{cases} \sin(4\pi x), & x \leq 0.5, \\ \sin(4\pi x) - 2.0, & x \geq 0.5, \end{cases}$$

and the initial data are

$$h(x, t = 0) = \begin{cases} \max(0, -0.5 - z(x)), & x \leq 0.5, \\ \max(0, -1.5 - z(x)), & x \geq 0.5, \end{cases} \quad u(x, t = 0) = 0.$$

The numerical solutions computed by the three HR schemes with 50 cells and final time $t = 0.5$ are shown in Figure 4. All schemes are well balanced up to machine accuracy.
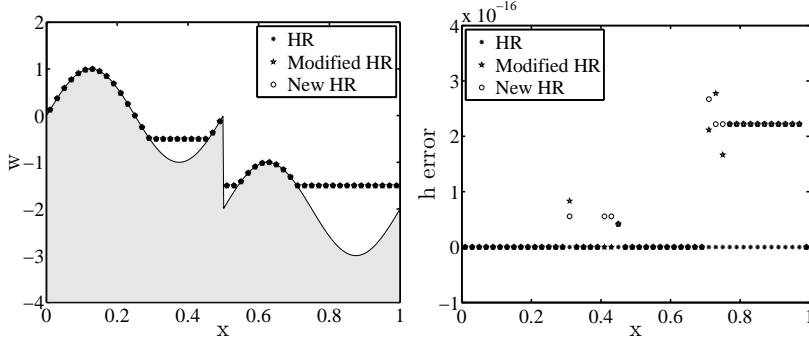
FIG. 4. *Still water over complex topography for* 50 *uniform cells,* $t = 0.5$. *Left: water level. Right: error of water height.*

5.3. Downhill flow over a sloped bottom. This test problem was introduced by Delestre et al. [10] to demonstrate a subtle difficulty of Audusse's original HR scheme. It was subsequently used by Morales et al. [15] to demonstrate the advantage of a modified HR scheme.

In the interval $[0, 3]$, the bottom is defined by

$$z(x) = -\frac{\alpha}{100}x$$

for different values of slope α ranging from 16 to 21. The initial condition is

$$h(x, t = 0) = 0.02, \quad u(x, t = 0) = 0.5.$$

The left inflow boundary is given by setting $h(x = 0, t) = 0.02$ and $u(x = 0, t) = 0.5$, and an outflow flow boundary condition is imposed at the right boundary $x = 3$. The simulations are performed until a steady state is reached at time $t = 10$.

As observed in [10], the water height of the HR scheme remains independent of the slope (see the top-left plot in Figure 5). This is contrary to the physical solution, for which the water level decreases with increasing downhill slope. The results for the modified HR scheme (top-right plot) and the present scheme (bottom-left plot) depend on the slope, but in slightly different ways. In the bottom-right plot, we compare the three schemes with a resolved reference solution for $\alpha = 21$. The advantages of the modified and especially the new HR schemes are clearly visible.

The following argument, along the lines of Remark 3.6, illuminates the situation. Let

$$S_{i+\frac{1}{2}} := S_{i+\frac{1}{2}-} + S_{i+\frac{1}{2}+}$$

be the total source term at interface $x_{i+\frac{1}{2}}$. Suppose that the slope is downward, $z_x < 0$, and the water height h is constant. The exact source term is given by

$$S_{i+\frac{1}{2}}^{\text{ex}} = -\frac{g}{\Delta x} \int_{x_i}^{x_{i+1}} h z_x \, dx = -g h z_x.$$
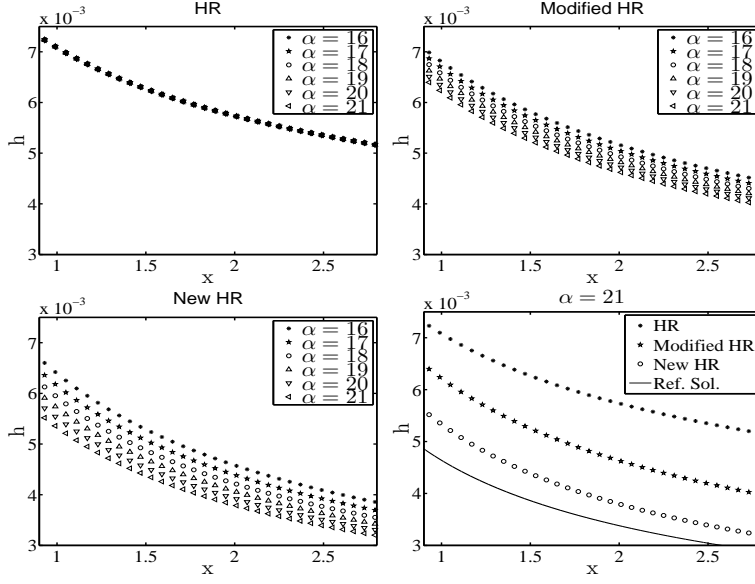
FIG. 5. *Flow down a linear slope with $h_l = 0.02$ and $u_l = 0.5$. Top left: HR. Top right: modified HR. Bottom left: new HR (all using 50 cells and $\alpha = 16, \ldots, 21$). Bottom right: comparison with the reference solution for $\alpha = 21$.*

In the fully wet case (labeled "fw" below), where all schemes coincide, (2.7)–(2.8) give

$$S_{i+\frac{1}{2}}^{\mathrm{fw}} = \frac{g}{2\Delta x}\left((h_{i+\frac{1}{2}-}^{\mathrm{AUD}})^2 - (h_i)^2 + (h_{i+1})^2 - (h_{i+\frac{1}{2}+}^{\mathrm{AUD}})^2\right)$$

$$= -\frac{g}{\Delta x}h_{i+1}(z_{i+1} - z_i) - \frac{g}{2\Delta x}(z_{i+1} - z_i)^2$$

$$= S_{i+\frac{1}{2}}^{\mathrm{ex}} - \frac{\Delta x\, g}{2}z_x^2.$$

In the partially wet case ($h < \Delta x|z_x|$), using (2.8)–(2.7) for Audusse's scheme, (2.14) for Morales' modification, and (2.17)–(2.18) for the present scheme, we obtain

$$S_{i+\frac{1}{2}}^{\mathrm{AUD}} = \frac{g}{2\Delta x}(h_{i+1})^2 = \frac{g}{2\Delta x}h^2,$$

$$S_{i+\frac{1}{2}}^{\mathrm{MOR}} = -\frac{g}{2\Delta x}\,h_{i+1}\left(z_{i+1} - z_{i+\frac{1}{2}}^{\mathrm{MOR}}\right) = -\frac{g}{2}\,h\,z_x,$$

$$S_{i+\frac{1}{2}}^{\mathrm{CN}} = -\frac{g}{2\Delta x}\left((h_i + h_{i+\frac{1}{2}-}^{\mathrm{CN}})(z_{i+\frac{1}{2}}^{\mathrm{CN}} - z_i) + (h_{i+\frac{1}{2}+}^{\mathrm{CN}} + h_{i+1})(z_{i+1} - z_{i+\frac{1}{2}}^{\mathrm{CN}})\right)$$

$$= -\frac{g}{2\Delta x}\left(2h_i(z_{i+1} + h_{i+1} - z_i) + h_{i+1}(-h_{i+1})\right)$$

$$= S_{i+\frac{1}{2}}^{\mathrm{ex}} - \frac{g}{2\Delta x}h^2.$$

It is instructive to introduce the ratio of the water height over the height increment:

$$\beta := h/(\Delta x|z_x|).$$

Then, in the fully wet case,

$$S_{i+\frac{1}{2}}^{\mathrm{fw}}/S_{i+\frac{1}{2}}^{\mathrm{ex}} = 1 - \frac{1}{2\beta},$$

which tends to the optimal value, 1, for deep water, while in the partially wet cases,

$$S_{i+\frac{1}{2}}^{\text{AUD}}/S_{i+\frac{1}{2}}^{\text{ex}} = \frac{\beta}{2}, \quad S_{i+\frac{1}{2}}^{\text{MOR}}/S_{i+\frac{1}{2}}^{\text{ex}} = \frac{1}{2}, \quad \text{and} \quad S_{i+\frac{1}{2}}^{\text{CN}}/S_{i+\frac{1}{2}}^{\text{ex}} = 1 - \frac{\beta}{2}.$$

Only for the present HR scheme does this fraction tend to the correct value of unity as the water height tends to zero. The values S/Sex are displayed against β in Figure 6.
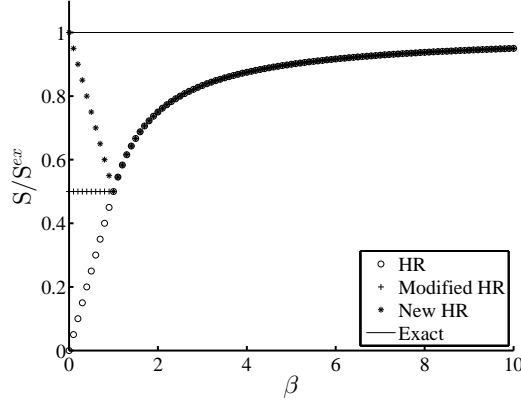
FIG. 6. S/S^{ex} for the exact source term ("—"), the original HR ("o"), the modified HR ("+"), and the new HR ("*"). Only the latter is consistent as $\beta \to 0$.

In the present experiment, β is not constant, but its value is approximately

$$\beta \approx \frac{0.01}{\frac{3}{50}\frac{20}{100}} = \frac{5}{6}.$$

To highlight the differences between the three schemes even further, we repeat the experiment with a value $\beta \approx \frac{1}{6}$ by setting the initial water height to $h = 0.004$. The results are displayed in Figure 7. As can be seen from the bottom-right part of the figure, the new HR scheme produces almost the exact solution on a grid of 50 cells, while the other two schemes do not.

5.4. Flow over a step. This test was introduced in [15, 8]. In the previous example, the bottom was continuous, and the fault of the HR scheme could be corrected by using a very fine mesh or higher order schemes.

Here, we consider the domain $[0, 1]$ with a sequence of six discontinuous bottoms given by

$$z(x) = \begin{cases} -0.1 & \text{for } x < 0.5, \\ z_r & \text{otherwise.} \end{cases}$$

and $z_r \in \{-0.2, -0.25, -0.3, -0.35, -0.4, -0.45\}$. The initial data are set to

$$h(x, t = 0) = 0.1, \quad u(x, t = 0) = 1.5$$

uniformly over the whole domain. The final time is $t = 3.0$. To compute the reference solution, we introduce a continuous bottom as in (5.1), with layer width $\delta = 10^{-2}$ and 10^4 cells. Therefore, there are 100 cells in the layer.

It is easy to check that the interface at the discontinuity is partially wet, so Audusse's source term depends only on the water level to the right of the step, and
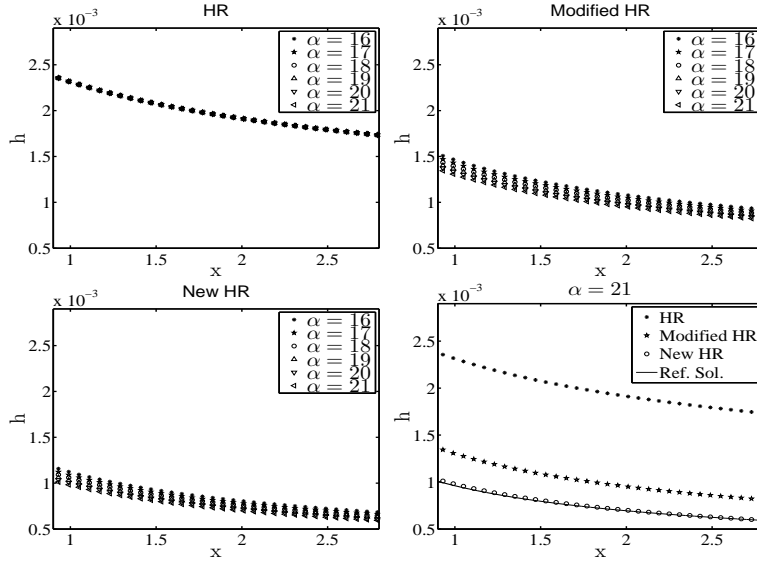
FIG. 7. *Flow down a linear slope with $h_l = 0.004$ and $u_l = 0.5$. Top left: HR. Top right: modified HR. Bottom left: new HR (all using 50 cells and $\alpha = 16, \ldots, 21$). Bottom right: comparison with the reference solution for $\alpha = 21$.*

not on the step size $z_r - z_l$. This is confirmed by the numerical results displayed in the top-left plot in Figure 8, which do not differ as the step size varies. Clearly, this does not reflect the increasing gravitational acceleration correctly.

The top-right and bottom-left plots of Figure 8 show that the error produced by the original HR method is corrected by both the modified HR method and the new HR method. As shown in these subfigures, the lower the right bottom z_r, the lower the water depth in the right region. On the other hand, we can also see from these subfigures that the numerical results from the two schemes are different; it is clear that the right water depth for the new HR method is lower than that for the modified HR method.

The results for the three schemes for the right bottom $z_r = -0.45$ are shown in the bottom-right subfigure, in particular in the zoom of that subfigure. All three water levels are above the reference solution. Compared with the size of the jump, the errors of the three HR schemes are 9.1%, 3.4%, and 0.6%.

5.5. Dam break over a dry step. Here we consider a dam break over a dry bottom, combined with a bottom step to the right of the dam break. Compared with the previous problem, the additional difficulty is the wet-dry front propagating to the right. This problem has been considered in [8, 5]. The domain is $[0, 1]$, and the bottom is defined by

$$z(x) = \begin{cases} -0.1 & \text{for } x < 0.1, \\ -0.45 & \text{otherwise.} \end{cases}$$

The initial data are

$$u(x) = 0, \quad h(x) = \begin{cases} 0.5 & \text{for } x < 0.05, \\ 0 & \text{otherwise.} \end{cases}$$
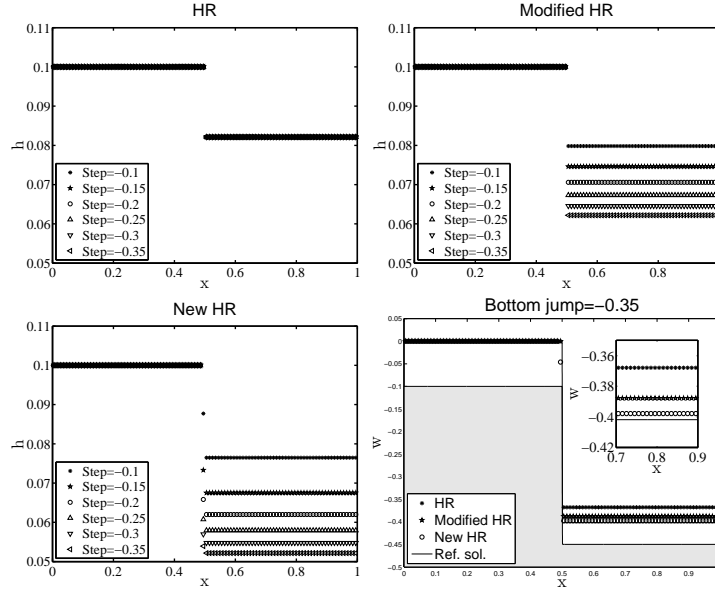
FIG. 8. *Downhill flow over a step. Water depths computed with HR (top left), modified HR (top right) and new HR (bottom left) schemes with several different bottom steps and 100 cells. Bottom right: water levels of all three schemes for $z_r = -0.45$ compared with the reference solution (including a zoom).*

The final time is $t = 0.18$. We compute the reference solution using (5.1), $\delta = 10^{-3}$, and 10^5 cells.

In Figure 9, we display the front positions, the velocity histories, and the final solutions using 400 cells. While the fronts computed by all three schemes lag behind the reference solution, the new HR scheme is clearly superior to the previous ones at and away from the front.

5.6. Flow against a step. Here we consider flow towards, and sometimes over, a rising step [15]. From our derivation, there is no particular reason why the new HR scheme should be superior to the previous ones, and indeed our experiments only confirm that the performance is comparable.

We consider the domain $[-5, 5]$ and a series of test cases with steps of various decreasing heights:

$$z(x) = \begin{cases} -0.8 & \text{for } x < 0.5, \\ z_r & \text{otherwise,} \end{cases}$$

where $z_r = -0.4, -0.5, -0.65, -0.75$. The initial height and velocity are

$$h(x, t = 0) = 0.1, \quad u(x, t = 0) = 1.5 \quad \text{for all} \quad x \in [-5, 5].$$

The final time is $t = 4.5, 3.5, 2.0, 5.0$. Here we compute the reference solution using (5.1), $\delta = 10^{-2}$, and 10^5 cells. The numerical results for the three HR schemes with 100 cells are shown in Figure 10.

For all cases, the original and the present HR method give similar results very close to the reference solution. The modified HR scheme produces an undershoot of
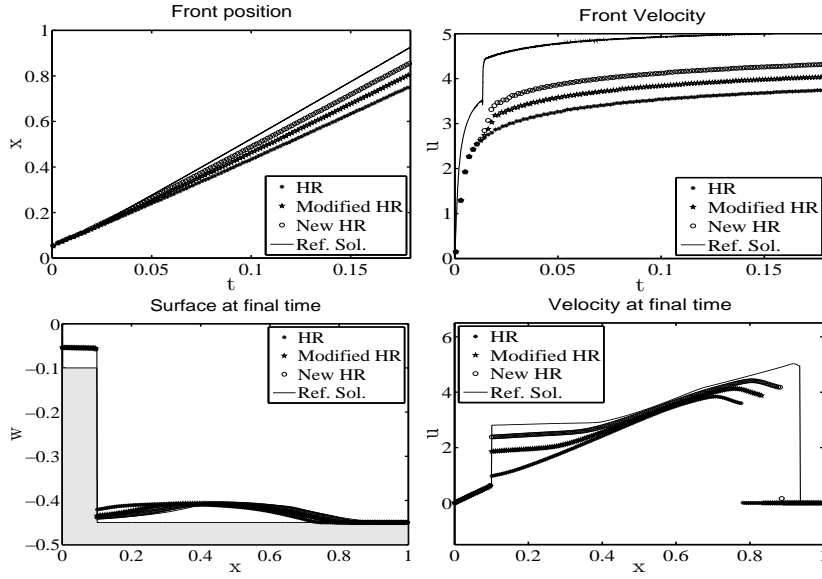
FIG. 9. *Dam break over dry bottom followed by a downhill step. Top: front positions and front velocity histories. Bottom: water level and velocity at final time.*
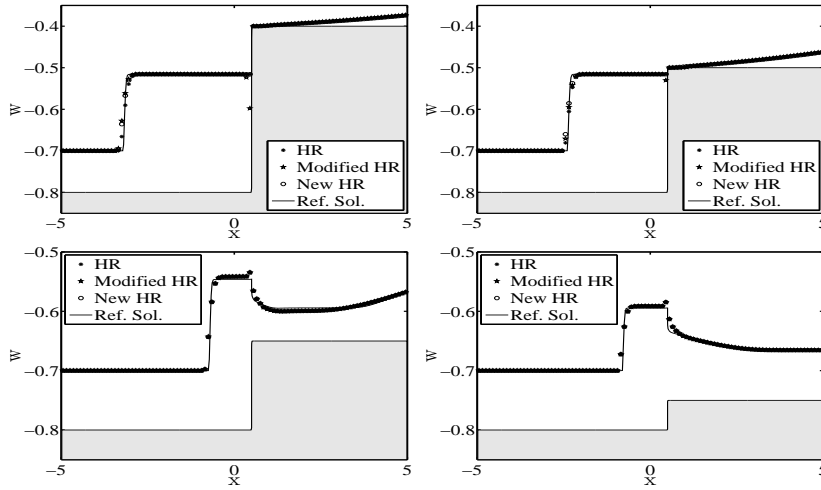

FIG. 10. *Water levels for flow against steps of size* 0.4, 0.3, 0.15, *and* 0.05.

the water height adjacent to the discontinuity, which disppears as the height of the step decreases.

6. Conclusions. We have introduced a new hydrostatic reconstruction (HR) scheme for the shallow water equations using the technique of subcell reconstructions. In singular layers, where both the conservative variables and the bottom topography are discontinuous, the nonconservative product is separated according to a natural definition of the bottom topography in the presence of an embedded wet-dry front. An intermediate water height is defined to the left and to the right of the front, and

the source term can then be evaluated. This construction only affects a few lines of code of the original HR scheme [2]. The subcell reconstruction via singular layers simplifies and clarifies the derivation of the classical HR schemes, and it can be used to design future schemes.

We have proved positivity of the water height, well-balancing of the lake at rest, and a semidiscrete entropy inequality for our scheme. For a number of challenging downhill flows studied recently in the literature, the new scheme yields superior results.

Appendix A. Summary of the new HR scheme.   The first order time-explicit new HR scheme is given by

$$U_i^{n+1} := U_i^n - \frac{\Delta t}{\Delta x}\big(F_{i+\frac{1}{2}} - F_{i-\frac{1}{2}}\big) + \Delta t\big(S_{i-\frac{1}{2}+} + S_{i+\frac{1}{2}-}\big)$$

with conservative fluxes $F_{i+\frac{1}{2}} := \mathcal{F}(U_{i+\frac{1}{2}-}, U_{i+\frac{1}{2}+})$ (see section 2.4 for the conditions on the numerical flux) and interface source terms given by

$$S_{i+\frac{1}{2}-}^{(h)} := 0, \quad S_{i+\frac{1}{2}-}^{(hu)} := -g\,\frac{h_i + h_{i+\frac{1}{2}-}}{2}\,\frac{z_{i+\frac{1}{2}} - z_i}{\Delta x},$$

$$S_{i+\frac{1}{2}+}^{(h)} := 0, \quad S_{i+\frac{1}{2}+}^{(hu)} := -g\,\frac{h_{i+\frac{1}{2}+} + h_{i+1}}{2}\,\frac{z_{i+1} - z_{i+\frac{1}{2}}}{\Delta x}.$$

The vectors of conservative variables $U_{i+\frac{1}{2}\pm}$ are given by

$$U_{i+\frac{1}{2}-} := \begin{pmatrix} h_{i+\frac{1}{2}-} \\ h_{i+\frac{1}{2}-}u_i \end{pmatrix}, \; U_{i+\frac{1}{2}+} := \begin{pmatrix} h_{i+\frac{1}{2}+} \\ h_{i+\frac{1}{2}+}u_{i+1} \end{pmatrix},$$

with water heights

$$h_{i+\frac{1}{2}-} := \min(w_i - z_{i+\frac{1}{2}}, h_i), \quad h_{i+\frac{1}{2}+} := \min(w_{i+1} - z_{i+\frac{1}{2}}, h_{i+1}),$$

water levels $w_i := z_i + h_i$, and intermediate bottom

$$z_{i+\frac{1}{2}} := \min\big(\max(z_i, z_{i+1}), \min(w_i, w_{i+1})\big).$$

REFERENCES

[1] R. ABGRALL AND S. KARNI, *A comment on the computation of non-conservative products*, J. Comput. Phys., 229 (2010), pp. 2759–2763.

[2] E. AUDUSSE, F. BOUCHUT, M.-O. BRISTEAU, R. KLEIN, AND B. PERTHAME, *A fast and stable well-balanced scheme with hydrostatic reconstruction for shallow water flows*, SIAM J. Sci. Comput., 25 (2004), pp. 2050–2065.

[3] D. S. BALE, R. J. LEVEQUE, S. MITRAN, AND J. A. ROSSMANITH, *A wave propagation method for conservation laws and balance laws with spatially varying flux functions*, SIAM J. Sci. Comput., 24 (2002), pp. 955–978.

[4] A. BERMUDEZ AND M. E. VAZQUEZ, *Upwind methods for hyperbolic conservation laws with source terms*, Comput. & Fluids, 23 (1994), pp. 1049–1071.

[5] A. BOLLERMANN, G. CHEN, A. KURGANOV, AND S. NOELLE, *A well-balanced reconstruction of wet/dry fronts for the shallow water equations*, J. Sci. Comput., 56 (2013), pp. 267–290.

[6] F. BOUCHUT, *Nonlinear Stability of Finite Volume Methods for Hyperbolic Conservation Laws and Well-Balanced Schemes for Sources*, Frontiers in Mathematics, Birkhäuser, Basel, 2004.

[7] M. J. CASTRO, J. M. GALLARDO, AND C. PARÉS, *High order finite volume schemes based on reconstruction of states for solving hyperbolic systems with nonconservative products. Applications to shallow-water systems*, Math. Comp., 75 (2006), pp. 1103–1134.

[8] M. J. Castro, P. G. LeFloch, M. L. Muñoz-Ruiz, and C. Parés, *Why many theories of shock waves are necessary: Convergence error in formally path-consistent schemes*, J. Comput. Phys., 227 (2008), pp. 8107–8129.

[9] G. Dal Maso, P. G. LeEfloch, and F. Murat, *Definition and weak stability of nonconservative products*, J. Math. Pures Appl. (9), 74 (1995), pp. 483–548.

[10] O. Delestre, S. Cordier, F. Darboux, and F. James, *A limitation of the hydrostatic reconstruction technique for Shallow Water equations*, C. R. Math. Acad. Sci. Paris, 350 (2012), pp. 677–681.

[11] E. Godlewski and P.-A. Raviart, *Numerical Approximation of Hyperbolic Systems of Conservation Laws*, Applied Mathematical Sciences 118, Springer, New York, 1996.

[12] A. Harten, P. D. Lax, and B. van Leer, *On upstream differencing and Godunov-type schemes for hyperbolic conservation laws*, SIAM Rev., 25 (1983), pp. 35–61.

[13] A. Kurganov and D. Levy, *Central-upwind schemes for the Saint-Venant system*, ESAIM Math. Model. Numer. Anal., 36 (2002), pp. 397–425.

[14] P. D. Lax and B. Wendroff, *Systems of conservation laws*, Comm. Pure Appl. Math., 13 (1960), pp. 217–237.

[15] T. Morales de Luna, M. J. Castro Díaz, and C. Parés, *Reliability of first order numerical schemes for solving shallow water system over abrupt topography*, Appl. Math. Comput., 219 (2013), pp. 9012–9032.

[16] M. L. Muñoz-Ruiz and C. Parés, *On the convergence and well-balanced property of path-conservative numerical schemes for systems of balance laws*, J. Sci. Comput., 48 (2011), pp. 274–295.

[17] S. Noelle, N. Pankratz, G. Puppo, and J. R. Natvig, *Well-balanced finite volume schemes of arbitrary order of accuracy for shallow water flows*, J. Comput. Phys., 213 (2006), pp. 474–499.

[18] S. Noelle, Y. Xing, and C.-W. Shu, *High-order well-balanced finite volume WENO schemes for shallow water equation with moving water*, J. Comput. Phys., 226 (2007), pp. 29–58.

[19] S. Noelle, Y. Xing, and C.-W. Shu, *High-order well-balanced schemes*, in Numerical Methods for Relaxation Systems and Balance Equations, Quaderni di Matematica, Dipartimento di Matematica, Seconda Universita di Napoli, Naples, Italy, 2009.

[20] C. Parés, *Numerical methods for nonconservative hyperbolic systems: A theoretical framework*, SIAM J. Numer. Anal., 44 (2006), pp. 300–321.

[21] P. L. Roe, *Approximate Riemann solvers, parameter vectors, and difference schemes*, J. Comput. Phys., 43 (1981), pp. 357–372.

[22] E. F. Toro, *Riemann Solvers and Numerical Methods for Fluid Dynamics*, Springer, Berlin, 1999.

[23] J. G. Zhou, D. M. Causon, C. G. Mingham, and D. M. Ingram, *The surface gradient method for the treatment of source terms in the shallow-water equations*, J. Comput. Phys., 168 (2001), pp. 1–25.